Geophys. J. R. astr. Soc. (1972) **29**, 49–64.

An Array Experiment with Magnetic Variometers Near the Coasts of South-east Australia

F. E. M. Lilley and D. J. Bennett

(Received 1972 January 27)

Summary

An array of magnetic variometers has been operated in the south-east corner of the Australian mainland, observing the coast effect simultaneously in two dimensions for the first time. The observations are presented as sets of variograms in the time domain and as contour maps of certain parameters in the frequency domain. Vertical field response functions are determined for each station, and the concept of fitting a surface over the area, using the response functions to define tangential planes, is introduced.

By choosing different polarizations of the horizontal fields, the effects of the two coast lines, which are approximately at right angles to one another, can be distinguished. A major result is that for the East Coast, the enhanced vertical variations are not accompanied by significantly enhanced horizontal variations. The distinctive coast effect of the Bass Strait is noted, especially concerning the amplitude of the variations in the horizontal fields. There is a suggestion of an anomalous region in western Victoria, which may correlate with the 'Newer Volcanics' rock structure of the area. A quantitative interpretation is planned for a subsequent paper.

Introduction

This paper describes observations from an experiment held during the first half of 1971, in which an array of instruments recording transient geomagnetic variations was kept in operation across south-east Australia, from the Great Australian Bight to the Tasman Sea. It is the first such array experiment to be reported from Australia, though it was actually the second to be carried out there. An earlier one was conducted across south central Australia in 1970, (Gough, McElhinny & Lilley, in preparation).

The area covered by the experiment is shown in Fig. 1. There are several reasons for conducting a geomagnetic depth sounding experiment in south-east Australia. Firstly, a number of high heat flows have been measured in the area, both in the Highlands Fold Belt of the Tasman geosyncline to the east, and in the 'Newer Volcanics' of Victoria to the west, (Jaeger 1970). Volcanic activity in the latter area has been dated to as recently as 6000 yr BP (Gill 1967). It is possible that remnants of the magma chambers will still be at elevated temperatures, and the principle of mapping higher temperatures in the crust and upper mantle through their consequence of higher electrical conductivity has been one of the longstanding interests of geomagnetic deep sounding.

Secondly, of the seven array studies which had been made since Gough & Reitzel (1967) first developed an instrument which could be economically reproduced in

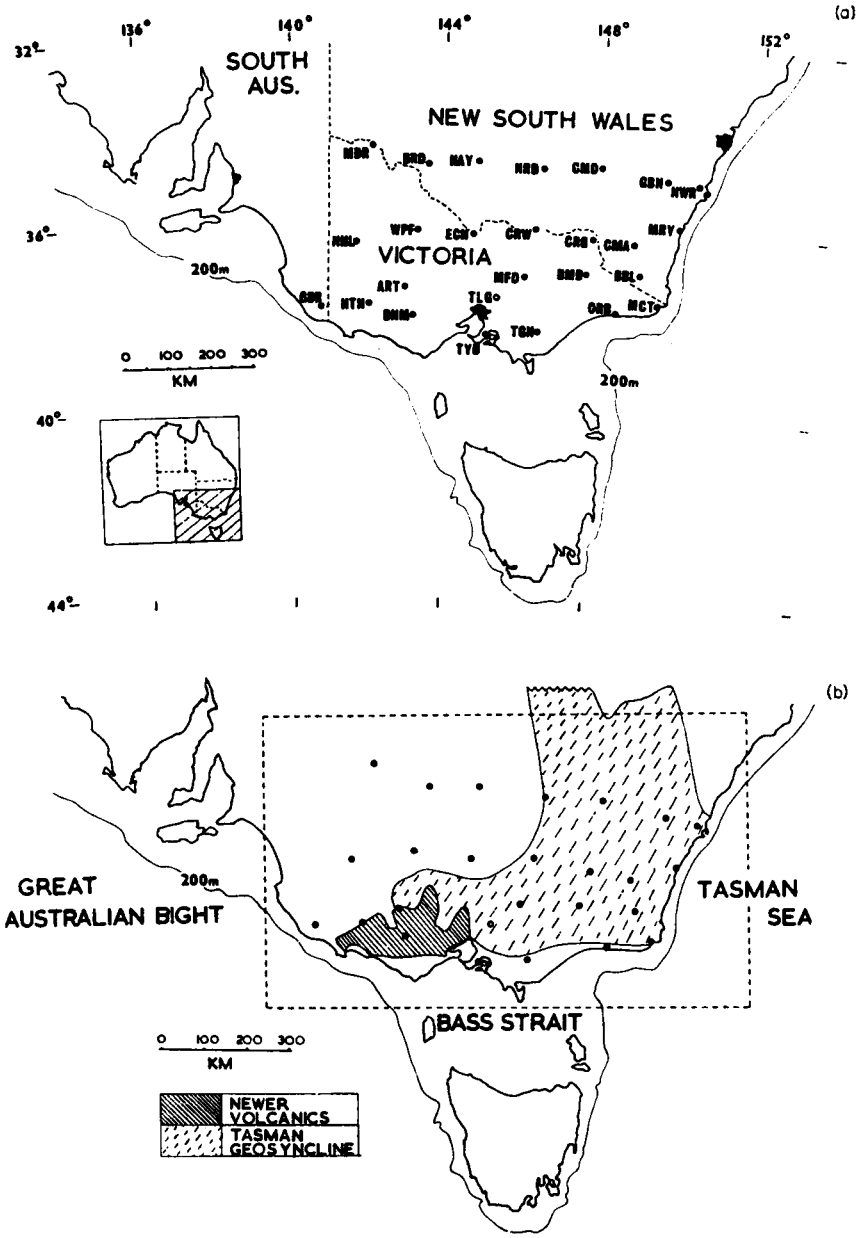

FIG. 1(*a*) Map of the observing sites; (*b*) Major tectonic features in the array area. The rectangle drawn around the observing sites is the frame for all subsequent array diagrams.

large sets, up to the time in question all had been remote from coasts. It was therefore of interest to carry out an array study near a coast, to see if the extra information from recording the variation fields over a two-dimensional area, rather than along a one-dimensional line, could help in clarifying the cause of the enhancement of vertical variations near coast lines. This is the phenomenon known as the coast-effect; it was first described by Parkinson (1959).

An array study for this purpose might be especially rewarding because good control may be hoped for over the variation fields of all three geomagnetic components, and as pointed out by Bullard & Parker (1971), the horizontal components of the coast effect may be particularly diagnostic as to its cause.

The experiment

Twenty-five variometers of the Gough–Reitzel type were installed at airstrips, at sites shown in Fig. 1. The twenty-sixth station of Fig. 1 is the permanent observatory Toolangi, (TLG), for which the records are published with the permission of the Director of the Australian Bureau of Mineral Resources. The portable instruments were installed and retrieved by a road party, and serviced in the interim by light aircraft: an ideal mode of transport for the purpose. The instruments were completely buried and operated unattended between servicing visits (every three weeks). A high degree of successful recording time was returned, and the instruments were calibrated at the start and again at the finish of every service visit.

During the observing period, 1971 February 3 to May 15, a variety of magnetic activity occurred. The data of this paper are based upon two particular periods of activity, which were chosen as optimum events for analysis. The times of the events were March 19, 1100–1800, and April 11, 0800–1800. The instruments recorded the three variation components H (magnetic north), D (magnetic east), and Z (vertically down), but because the magnetic declination ranges over some four degrees across the array, it was decided to work with the alternative horizontal components of X (geographic north) and Y (geographic east). The corresponding sets of X, Y and Z variograms are presented in Figs 2 and 3.

Data reduction

The original records being on photographic film, a certain amount of manipulation was necessary to reduce them to digital form. This part of the data analysis follows that given in the first such array study, by Reitzel *et al.* (1970). The steps taken were the printing of ($\times 10$) enlargements of the sections of the data film of interest; and then semi-automatic digitization of these enlargements. The data were adjusted for the calibration constants of the individual instruments, and corrected for a minor interaction between two of the sensing elements, in each case. Series for X and Y were computed from those for H and D. The frequency spectra were obtained by direct Fourier transformation; the data series of interest was multiplied by a $\sin^2$ taper over its first and last 10 points, and a linear trend removed. Sections of the variograms which could be considered as complete individual transients were chosen for analysis, so that the whole of the frequency spectrum obtained by transforming them could be taken to be valid. This is in contrast to the analysis of a time series which has clearly suffered serious truncation, and in this sense the study of geomagnetic events such as bays is fortunate, in that the whole disturbance may frequently be analysed complete.

Zeros could be added to increase the length of a time series, without altering the frequency spectrum of the event. Fourier transformation of such a longer time series results in finer definition of the frequency spectrum, and representative spectra are

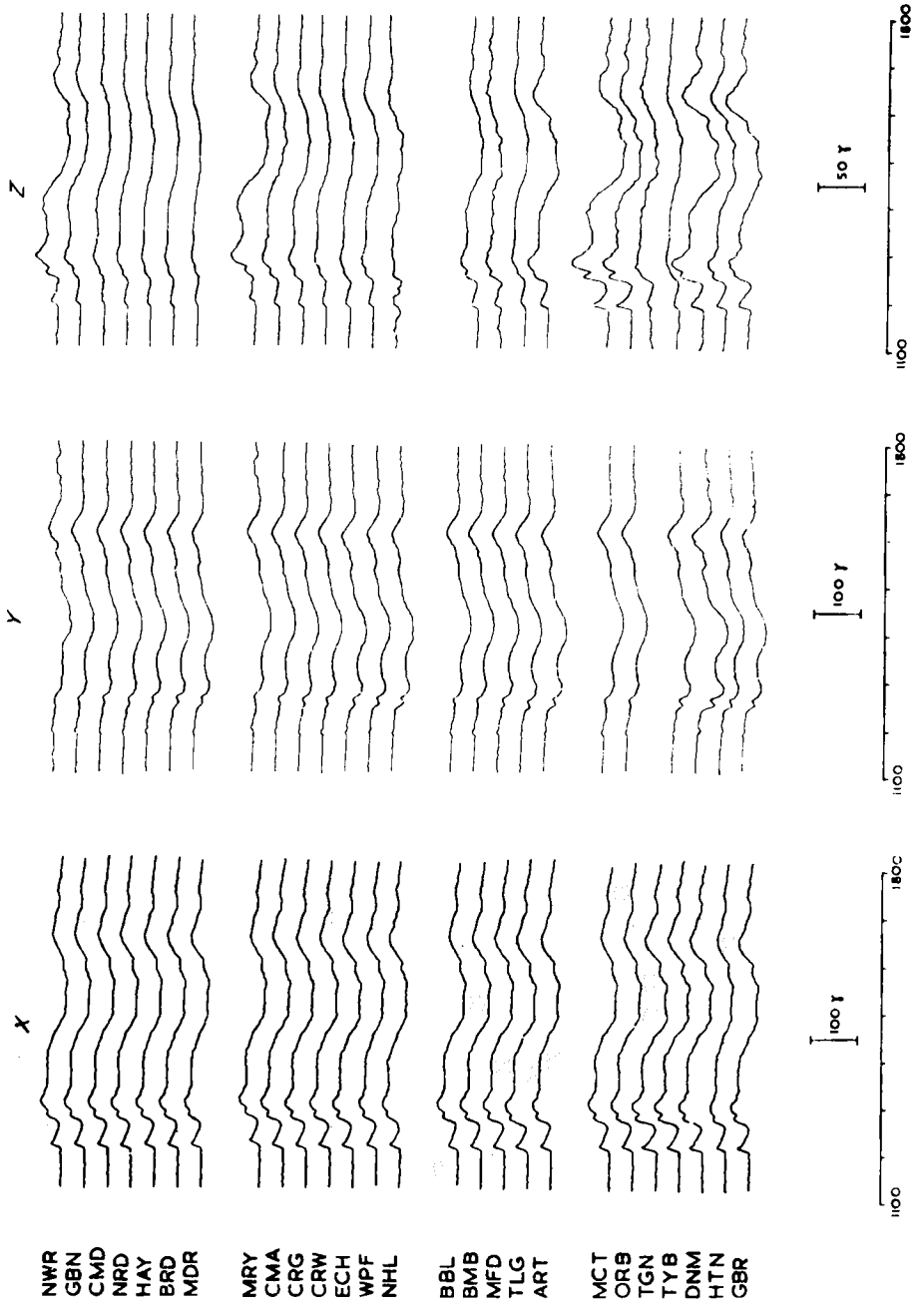

FIG. 2. Variograms for the event of 1971 March 19.

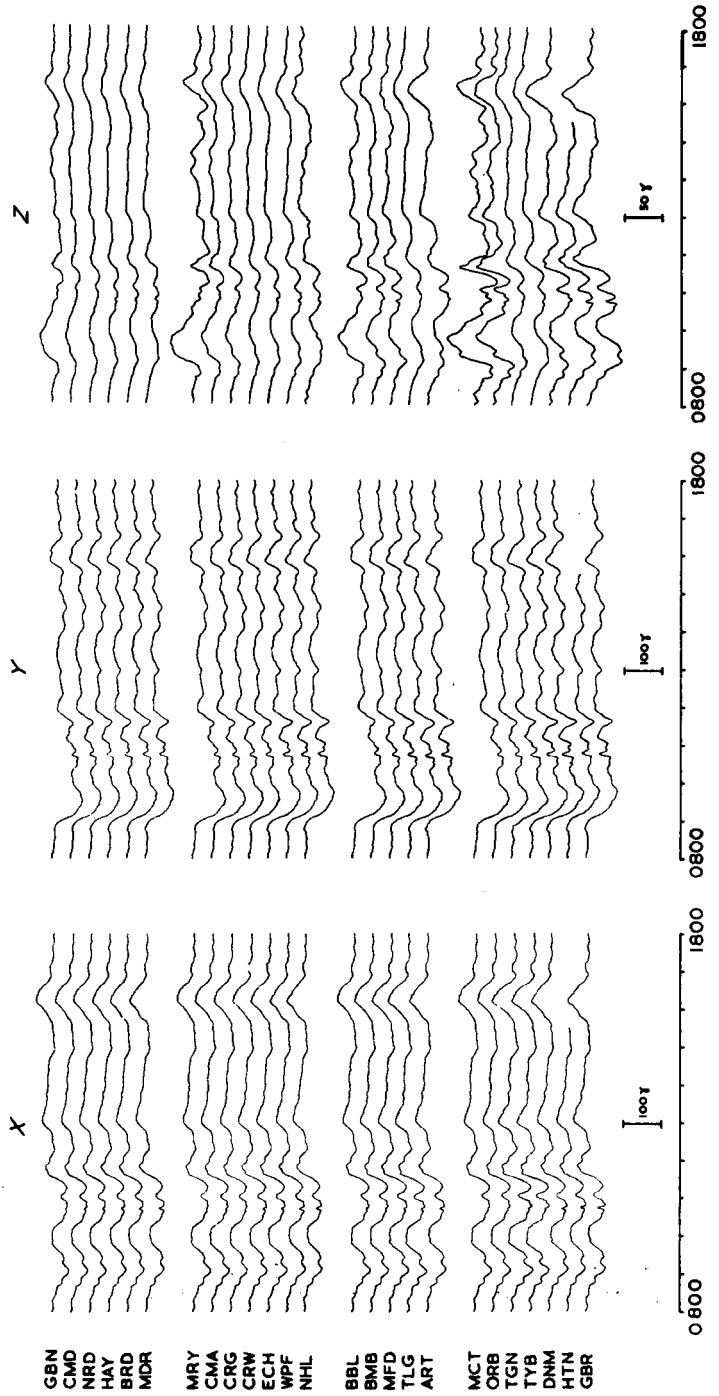

FIG. 3. Variograms for the event of 1971 April 11.

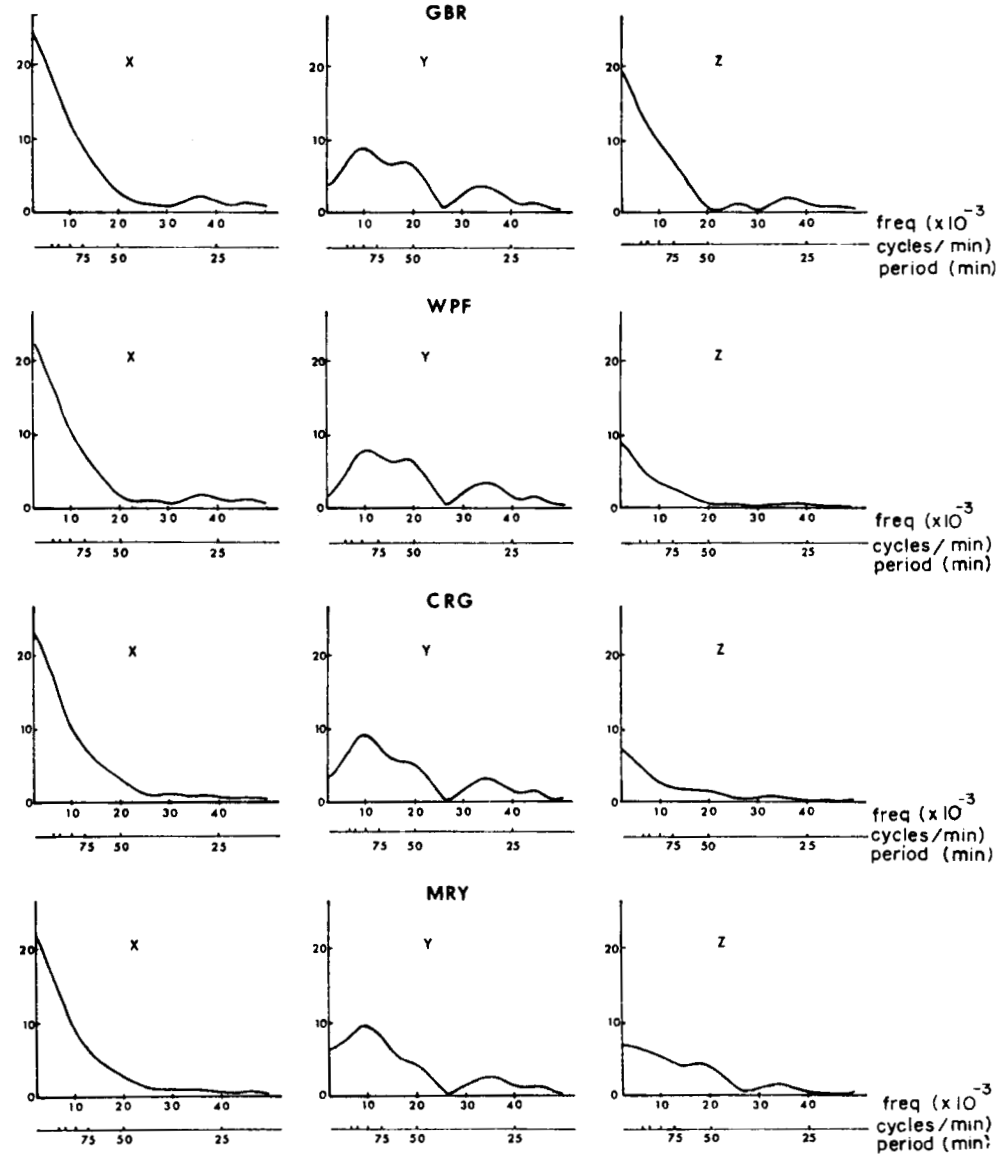

FIG. 4. Spectra of four stations for the event of 1971 April 11, 1500–1800 hr. Spectral amplitudes are in units of 90 gamma/cycle/min.

presented in Fig. 4. Particular frequencies and polarizations were chosen, and for these the Fourier transform parameters of amplitude and phase were plotted on base maps, and contoured. Representative examples of these are presented in the next section.

Polarization parameters for the horizontal variations were calculated following the monochromatic theory of Born & Wolf (1959). A summary of the relevant formulae follows, (adapted for the fact that the $X-Y$ axes of geomagnetism are reversed from the usual configuration taken for 2-dimensional $x-y$ axes).

If a disturbance has horizontal components of

$$X = a_2 \cos(\omega t + \delta)$$

$$Y = a_1 \cos \omega t$$

then the point (X, Y) traces out an ellipse with the passage of time.

Define α, $(0 \leqslant \alpha \leqslant \pi/2)$ such that

$$\tan \alpha = \frac{a_2}{a_1} \quad .$$

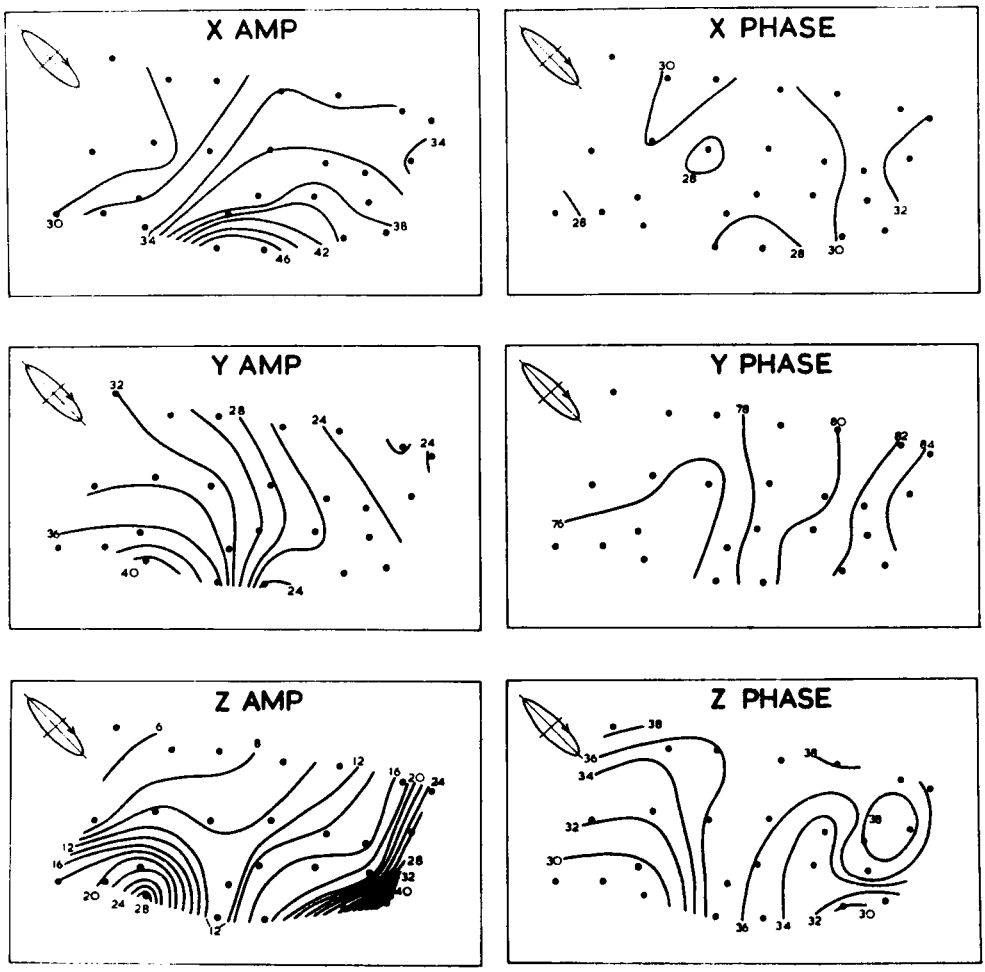

FIG. 5. Fourier transform parameter maps for 1971 March 19, 1215–1515 hr, at period 81·9 min, with ellipse of horizontal polarization. Units of phase are minutes; units of amplitude are 21 gamma/cycle/min.

The principle semi-axes a and b of the ellipse and the angle ψ, $(0 \leqslant \psi < \pi)$ which the major axis makes anticlockwise with geographic east are specified by the formulae

$$a^2+b^2 = a_1^2+a_2^2$$
$$\tan 2\psi = (\tan 2\alpha)\cos\delta$$
$$\sin 2\chi = (\sin 2\alpha)\sin\delta$$

$$\begin{cases} 0 < \psi < \tfrac{1}{2}\pi \text{ if } \cos\delta > 0 \\ \tfrac{1}{2}\pi < \psi < \pi \text{ if } \cos\delta < 0 \\ \psi = 0 \text{ if } \cos\delta = 0 \text{ and } a_1 > a_2 \\ \psi = \tfrac{1}{2}\pi \text{ if } \cos\delta = 0 \text{ and } a_1 < a_2 \end{cases}$$

where χ, $(-\pi/4 < \chi \leqslant \pi/4)$ is an auxiliary angle which specifies the shape and orientation of the ellipse:

$$\tan\chi = \pm\frac{b}{a} \quad .$$

If $\sin\delta > 0$, the ellipse is described in a clockwise sense, and if $\sin\delta < 0$, anticlockwise. For $\sin\delta = 0$, or if either a_1 or a_2 is zero, the ellipse degenerates to a line of linear polarization.

The values a_1, a_2 and δ, as functions of the angular frequency ω, come from

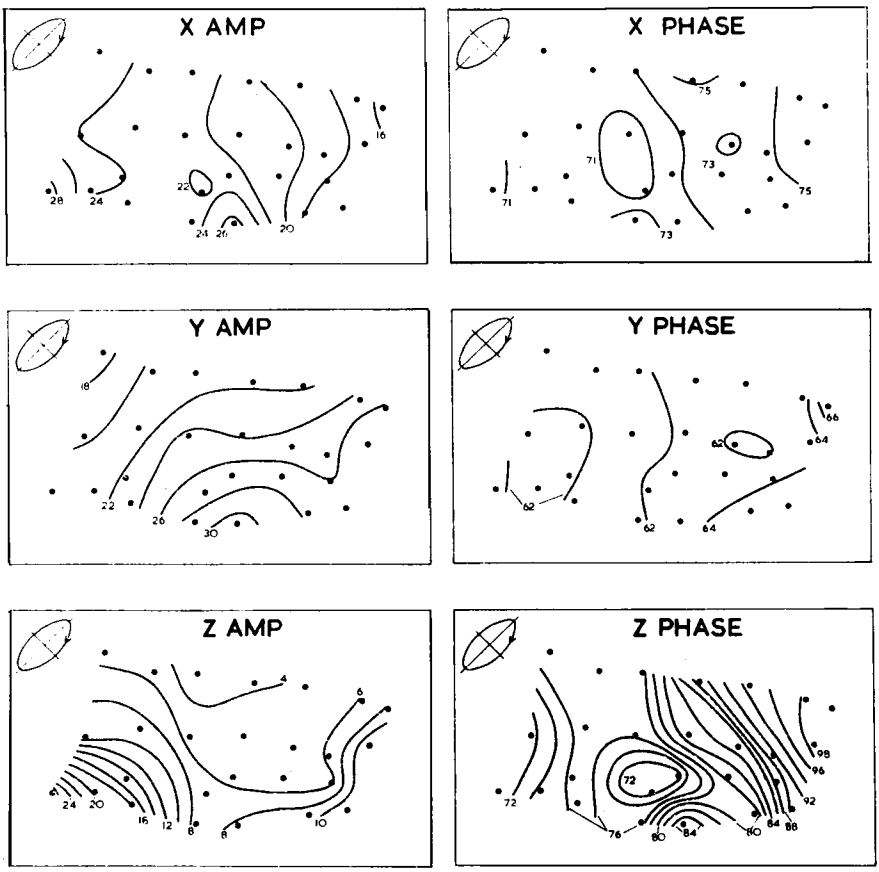

FIG. 6. Fourier transform parameter maps for 1971 March 19, 1500–1800 hr, at period 85·3 min, with ellipse of horizontal polarization. Units of phase are minutes; units of amplitude are 21 gamma/cycle/min.

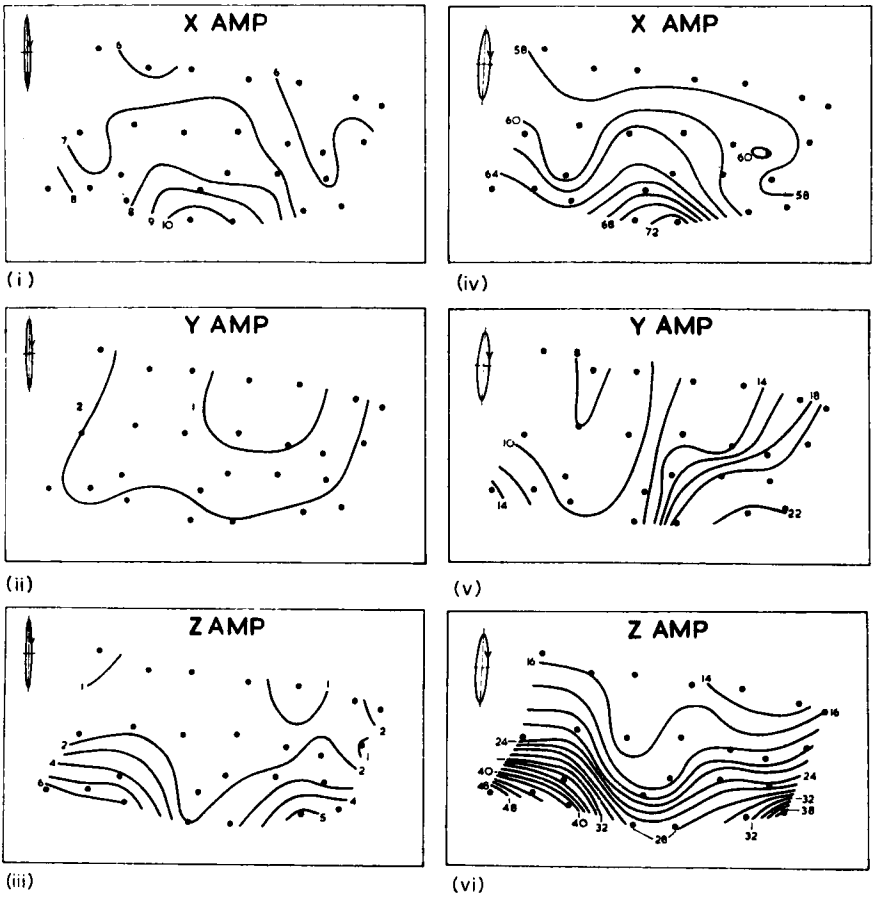

FIG. 7. (i)–(iii) Fourier transform parameter maps for 1971 March 19, 1500–1800 hr, at period 33·6 min. Units of amplitude are 21 gamma/cycle/min. (iv)–(vi) Fourier transform parameter maps for 1971 April 11, 1500–1800 hr, at period 186·2 min. Units of amplitude are 30 gamma/cycle/min. The ellipses shown are those of horizontal polarization.

Fourier transforms of selected events in the time domain. The particular definition of the Fourier transform adopted in this paper is

$$g(\omega) = \int_{-\infty}^{\infty} f(t) \exp(-i\omega t)\, dt \quad .$$

Results from spectral analysis

The parameters from the spectral analyses may be presented for any particular frequency in the form of contour maps. While it would be desirable, if possible, to use a frequency for which the spectra of the vertical components at all stations are at maxima, for a 3-dimensional conductivity structure there may be no reason to expect such general peaks to occur. The polarization characteristics of the horizontal variation fields are of crucial importance, and consequently the periods chosen have been decided upon largely for the sake of obtaining certain polarizations in the horizontal plane. This means many values have been taken which occur on the sides

of lobes in the computed frequency spectra, and the importance of a whole spectrum being valid is again emphasized.

Figs 5, 6 and 7 show a selection of the maps thus produced. The appropriate ellipse of polarization of the horizontal fields drawn on each one is for the central northern part of the area, that part most remote from the coasts. In most cases, data from BRD, HAY, NRD and ECH have been combined to give a representative ellipse. Thus Fig. 5, chosen for a period of maximum power in Z, shows the response of the area to a field polarized mainly southeast–northwest. Fig. 6 shows the response for a polarization mainly southwest–northeast, and Fig. 7 shows the response, for two different periods, to nearly linear north–south polarization. The significance of the maps will be further discussed below.

Station response functions and a ' response surface '

In geomagnetic variation studies, it is common to seek a fit of observed data to the equation

$$Z = AX + BY \tag{1}$$

where all quantities are functions of frequency. Z, X and Y have in-phase and quadrature components, and the response (or transfer) functions, A and B, are complex constants. Denoting the real and imaginary parts of a quantity by the subscripts r and i, equation (1) may be expanded as

$$Z_r = A_r X_r + B_r Y_r - A_i X_i - B_i Y_i \tag{2}$$

$$Z_i = A_r X_i + B_r Y_i + A_i X_r + B_i Y_r \tag{3}$$

These equations may be compared to the relationship first proposed by Parkinson (1959), who developed a graphical method equivalent to fitting

$$\Delta Z = A_p \Delta X + B_p \Delta Y \tag{4}$$

where ΔX, ΔY and ΔZ are actual in-phase changes of field over some successive time intervals, and A_p and B_p are real constants. Equation (4) defines a plane, and if data which satisfy this equation are plotted in a u, v, w cartesian co-ordinate system, (where the geometric u, v, w axes are parallel to the magnetic X, Y, Z axes), the horizontal component of the downwards normal to the plane which results is known as Parkinson's vector.

Equation (2) does not correspond exactly to equation (4), but estimates of A_r and B_r are commonly taken to represent A_p and B_p, and thus to define the Parkinson plane. A second plane, it is to be noted, is similarly defined by the imaginary components, A_i and B_i.

If observations are made at a number of closely-spaced stations, the determination of two particular planes at each one suggests the mapping of two surfaces over the area, to be defined by the simple condition that the planes at each station shall be parallel to the tangential planes of the surfaces there. The problem would be to determine surfaces

$$w_r = f_r(u, v) \quad \text{and} \quad w_i = f_i(u, v)$$

given

$$A_r = \frac{\partial f_r}{\partial u}, \; A_i = \frac{\partial f_i}{\partial u}, \; B_r = \frac{\partial f_r}{\partial v}, \; B_i = \frac{\partial f_i}{\partial v}$$

at every point where there is an observing station. Because A and B are functions of frequency, there will in fact be families of surfaces, corresponding to variation of the frequency value.

By power spectral analysis of the two periods of magnetic activity shown in Figs 2 and 3, estimates of A and B for each station were computed by a method essentially

Table 1

Station	Code	Geographic co-ords		Ar	Ai	Br	Bi
Ararat	ART	37° 19′ S	143° 00′ E	0·55	0·14	−0·12	0·09
Bombala	BBL	36° 55′	149° 11′	0·41	0·23	−0·05	−0·14
Benambra	BMB	36° 58′	147° 42′	0·37	0	−0·13	−0·06
Balranald	BRD	34° 36′	143° 34′	0·24	0·06	0	−0·02
Cooma	CMA	36° 18′	148° 58′	0·30	0·07	−0·23	−0·05
Cootamundra	CMD	34° 37′	148° 02′	0·21	0·06	−0·17	−0·04
Corryong	CRG	36° 11′	147° 53′	0·29	0·05	−0·15	−0·02
Corowa	CRW	35° 59′	146° 22′	0·24	0·11	−0·06	−0·03
Derrinallum	DNM	37° 54′	143° 11′	0·69	0·10	−0·13	−0·11
Echuca	ECH	36° 08′	144° 46′	0·25	0·10	0·04	−0·05
Goulburn	GBN	34° 49′	149° 44′	0·29	0·04	−0·32	−0·04
Mt Gambier	GBR	37° 44′	140° 46′	0·80	0·09	0·15	−0·03
Hay	HAY	34° 31′	144° 50′	0·19	0·02	−0·03	−0·06
Hamilton	HTN	37° 39′	142° 03′	0·70	0·09	0·01	0·01
Mallacoota	MCT	37° 36′	149° 43′	0·80	−0·12	−0·58	0·12
Mildura	MDR	34° 14′	142° 04′	0·20	0·11	0·04	−0·05
Mansfield	MFD	37° 02′	146° 08′	0·36	0·05	−0·08	−0·15
Moruya	MRY	35° 54′	150° 08′	0·46	0·03	−0·58	0·02
Nhill	NHL	36° 20′	141° 38′	0·33	0·11	0·16	−0·09
Narrandera	NRD	34° 42′	146° 31′	0·20	0·08	−0·07	−0·04
Nowra	NWR	34° 57′	150° 32′	0·54	0·04	−0·40	0·10
Orbost	ORB	37° 47′	148° 36′	0·71	−0·12	−0·22	−0·03
Traralgon	TGN	38° 12′	146° 28′	0·27	0·16	−0·04	−0·05
Toolangi	TLG	37° 33′	145° 28′	0·22	0·18	0·05	−0·01
Tyabb	TYB	38° 16′	145° 10′	0·26	0·14	0·12	−0·04
Wycheproof	WPF	36° 04′	143° 14′	0·35	0·08	−0·03	0·02

following that given by Everett & Hyndman (1967). These estimates are listed in Table 1 for the period of 80 min, which corresponds to Fig. 5. On the assumption that the real and imaginary parts of both A and B all have the same normal error distribution, a common standard deviation for all values has been estimated to be of order 0·3. (For Nowra and Bombala, for which only one period of magnetic activity was analysed, it is 0·5). Parkinson vectors computed from the real parts of the A and B values are plotted in Fig. 8. They are consistent with vectors for other sites in the area published previously by Parkinson (1959), Everett & Hyndman (1967), and Bennett & Lilley (1971).

The two surfaces which can be defined, everywhere tangential to the planes of the in-phase and quadrature response functions respectively, are by no means unique. As an experiment to determine one such surface for the in-phase response functions of Table 1, however, a polynomial was taken of degree just sufficiently high to exactly fit the observational data. Subsequent experience may provide different criteria for surface determination, but in the present exercise the coefficients a_{ij} were sought for the n^{th} degree surface,

$$w = \sum_{s=0}^{n} \sum_{r=0}^{s} a_{sr}\, u^{s-r}\, v^{r} \ . \tag{5}$$

The constant term a_{00} must remain undetermined, as for a surface defined entirely by the slope of tangential planes the zero level must be arbitrary.

Such a surface of degree n thus has $n(n+3)/2$ unknown coefficients to be calculated and each station gives two separate equations,

$$A_r = \frac{\partial w}{\partial u},\ B_r = \frac{\partial w}{\partial v}$$

for known u and v, the station coordinates of position. The number of stations needed to determine an n^{th} degree surface is thus the integral part of $[n(n+3)/2+1]/2$.

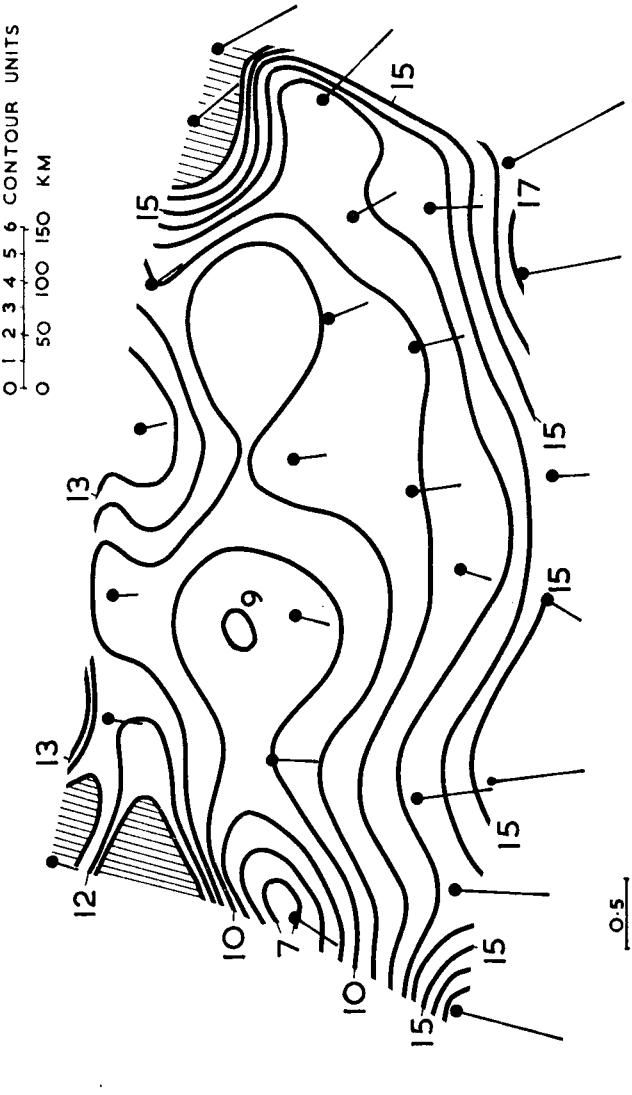

FIG. 8. Parkinson vectors for period 80 min, and the response surface fitted to them. The contour values are heights of the surface relative to an arbitrary zero level (and correspond to negative values of w as defined in the text).

Twenty-two stations are therefore sufficient for an eighth degree surface, and 27 stations would be needed for a ninth degree surface. To make full use of the data from the present 26 stations, the values of A_r and B_r as given in Table 1 were fitted to

$$A_r = \sum_{s=1}^{9} \sum_{r=0}^{5} (s-r)\, a_{sr}\, u^{s-r-1}\, v^r \tag{6}$$

$$B_r = \sum_{s=1}^{9} \sum_{r=0}^{5} r\, a_{sr}\, u^{s-r}\, v^{r-1} \tag{7}$$

with a_{94} and a_{95} arbitrarily set to zero, because 26 stations are not sufficient for a full ninth degree surface.

The coefficients a_{ij} were determined directly by solution of the 52 equations obtained from writing (6) and (7) for each of the observing sites. These coefficients were then used to generate a surface according to equation (5), and this is presented in Fig. 8 as a contour map, relative to an arbitrary zero level.The important problem of smoothing the surface has not been attempted, and in the two northern corners of the area there are steep undulations which have not been fully contoured.

The surface of Fig. 8 is just one of an infinite family which would fit the data, and it is presented as an example of how Parkinson vectors for a number of sites can be synthesized together. The advantage of such a map is that, unlike the maps of Figs 5, 6 and 7, it summarizes the response in the vertical field for all polarizations of variation in the horizontal field. If an optimum smoothed surface of this type were to be determined, it could be used to predict the vertical variations occurring at any point in the area, for any polarization of the horizontal fields.

The surface does not represent directly the level (or change in level) of any physical quantity in the area covered. However, in conjunction with a similar surface for A_i, B_i data, it contains in principle all information available from the analysis carried out so far. One method of interpretation might therefore aim at inverting such surfaces to give electrical conductivity distributions, especially if the surfaces have been determined using data from stations that were not occupied simultaneously. Indeed, an advantage of such surfaces is that their detail can be augmented by single station operation at subsequent times. However, when magnetic variation data right across such a large area has been recorded simultaneously, as in the present instance, it is in principle possible to separate the variations into normal and anomalous parts, (Porath, Oldenburg & Gough 1970). Further information, more valuable for interpretation purposes, may come from such a separation exercise, and one will be attempted in a subsequent paper.

The inter-relationships between the observed data, the polarization, the Parkinson vector, and the in-phase response surface may be seen by comparing the Z amplitude diagram of Fig. 5 with Fig. 8. The Parkinson vector points up the direction of steepest slope of the response surface, and a short vector corresponds to a small slope. At Echuca (ECH), for example, the component of the vector in the direction of the horizontal polarization is small: thus the slope in the response surface at that azimuth is low, and the Z amplitude observed is low. At Mallacoota (MCT), by contrast, the component of the Parkinson vector in the polarization direction is large, and the corresponding Z amplitude is high.

Discussion

The dominant feature of the results, in all the different forms of presentation, is the correlation of strong Z variation fields with the coastlines. The different polarizations of the horizontal fields in Figs 5, 6 and 7 distinguish the response of the different

coastlines one from the other. The Z response at the corner coastal station, Mallacoota, is particularly strong (see Figs 2 and 3).

The phase maps are generally less distinctive than the amplitude maps, and phases have been omitted for the almost linear polarizations of Fig. 7. However, the Z-phase of Fig. 6 has a distinctive and strong pattern, which may bear explanation. It can be seen that there is a total phase difference of 26 min across the map, corresponding to a quarter of a period. The reason for this becomes clear if the X and Y fields are considered resolved along the major and minor axes of the horizontal polarization ellipse, to give fields of X' and Y', say, as shown in Fig. 9. The X' and Y' fields will be $\frac{1}{2}\pi$ out of phase: the first, X', is almost perpendicular to the east coast, and the other, Y', is almost perpendicular to the coast near the south-west corner of the array. The Z phase map then rather clearly divides the Z amplitude response into a contribution from the east coast, in phase with the X' field, and a contribution from the south-west coast, in phase with the Y' field. A similar exercise for Fig. 5 is less productive, but the resolution of the horizontal fields into components parallel to the axes of polarization can be seen to have valuable applications, and it will be the subject of further investigation.

From the horizontal field maps of Figs 5 and 7 it is clear that for the east coast, adjoining the Tasman Sea, the very strong coast-effect in Z is accompanied by virtually no anomalous horizontal variations. The south-west coast, from the Bass Strait to the Great Australian Bight, shows a more complicated response. In Fig. 6, for a horizontal field polarized mainly perpendicular to it, the south-west coast shows the usual strong Z variation with negligible horizontal anomalous field. However for the other polarizations of Figs 5 and 7 a strong Z variation is still present, now with considerable strength also in the X and Y fields. Particularly striking, in Fig. 7, is the tendency for the Z contour lines to bow south into the Bass Strait while the X contour lines bow northwards inland.

In an area so strongly dominated by the coast effect, other anomalous responses, (of possible continental origin), may not be apparent so readily. However there is evidence of departure from the usual coast effect in the observations at the stations Hamilton (HTN), Derrinallum (DNM), and Ararat (ART), in the south-west corner of the array. Stronger horizontal variations are observed, and slightly stronger vertical variations, (see Fig. 5). The Parkinson vectors are deflected eastwards from the usual pattern, (see Fig. 8). It is possible that the effects are connected with the

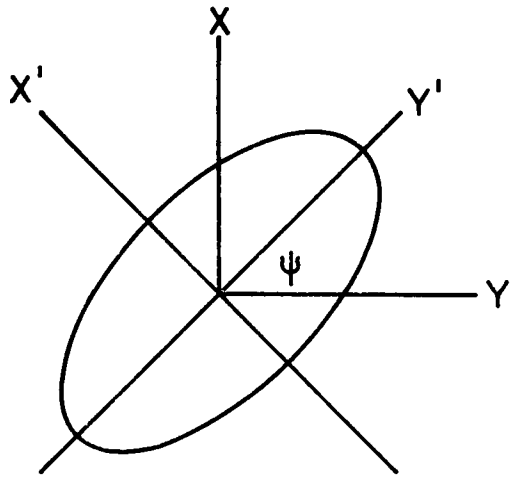

FIG. 9. Resolution of horizontal field components, X and Y, along directions parallel with the major and minor axes of the horizontal polarization ellipse.

higher heat flows of the Victoria ' Newer Volcanics ', (marked on Fig. 1(*b*)). However it will be necessary to interpret this anomaly in conjunction with the change in the coastline from one of deep ocean (the Great Australian Bight) to one of shallow seas (the Bass Strait) which occurs nearby.

Pending quantitative model fitting, a tentative interpretation of the main features of the maps may be summarized as follows. Strong coast effects are observed in the vertical fields near the edges of deep oceans, but not near the edge of a shallow sea (the Bass Strait). The strong vertical variations occur for horizontal fields polarized normally to a coast line, but they are not accompanied by anomalous horizontal variations. Near the south-west coast of Victoria there is a continental anomaly, which responds strongly in the vertical component when the horizontal fields are polarized approximately southeast–northwest. Anomalous variations in the horizontal fields also occur in this region. It is unlikely that such large horizontal field anomalies could be caused solely by a near surface effect, such as current channelling in the Bass Strait. Therefore both vertical and horizontal anomalous components could be connected with the high heat flow region of the nearby recent volcanics.

Acknowledgments

The exercise was made possible by the generosity of Professor D. I. Gough, who kindly lent his array of instruments to the authors, during the second half of his sabbatical visit to the Australian National University. He is thanked for his advice and assistance at all stages of the work.

Mr. P. M. McGregor assisted in locating the records for Toolangi. Many people gave valuable help during the field operations, especially the pilot, Mr. M. Thorpe.

One of the authors, (D.J.B.), is the recipient of a research scholarship awarded by the Australian National University.

Department of Geophysics and Geochemistry
Australian National University
Canberra

References

Bennett, D. J., & Lilley, F. E. M., 1971. The effect of the south-east coast of Australia on transient magnetic variations, *Earth Planet. Sci. Letts* **12**, 392–398

Born, Max & Wolf, Emil, 1959. *Principles of Optics*, p. 803, Pergamon Press Ltd, London.

Bullard, E. C. & Parker, R. L., 1971. Electromagnetic induction in the ocean, *The Sea*, Volume 4, pp. 695–730, ed. A. E. Maxwell, Wiley-Interscience, New York.

Everett, J. E. & Hyndman, R. D., 1967. Geomagnetic variations and electrical conductivity structure in south-western Australia, *Phys. Earth Planet Int.*, **1**, 24–34.

Gill, Edmund, D., 1967. Evolution of the Warrnambool—Port Fairy Coast and the Tower Hill Eruption, Western Victoria, pp. 340–364, *Landform studies from Australia and New Guinea*, eds J. N. Hennings and J. A. Mabbutt, Australian National University Press, Canberra, pp. 434, 1967.

Gough, D. I. & Reitzel, J. S., 1967. A portable three-component magnetic variometer, *J. Geomagn. Geoelect.*, Kyota, **19**, 203–215.

Jaeger, J. C., 1970. Heat flow and radioactivity in Australia, *Earth Planet. Sci. Lett.*, **8**, 285–292.

Parkinson, W. D., 1959. Direction of rapid geomagnetic fluctuations, *Geophys. J. R. astr. Soc.*, **2**, 1–14.

Porath, H., Oldenburg, D. W. & Gough, D. I., 1970. Separation of magnetic variation fields and conductive structures in the western United States, *Geophys. J. R. astr. Soc.*, **19**, 237–260.

Reitzel, J. S., Gough, D. I., Porath, H. & Anderson III, C. W., 1970. Geomagnetic deep sounding and upper mantle structure in the western United States, *Geophys. J. R. astr. Soc.*, **19**, 213–235.